analytical chemistry

ARTICLE

pubs.acs.org/ac

Copper Quantum Clusters in Protein Matrix: Potential Sensor of Pb^{2+} Ion

Nirmal Goswami,[†] Anupam Giri,[†] M. S. Bootharaju,[‡] Paulrajpillai Lourdu Xavier,[‡] Thalappil Pradeep,[*,‡] and Samir Kumar Pal[*,†]

[†]Department of Chemical, Biological and Macromolecular Sciences, S. N. Bose National Centre for Basic Sciences, Block JD, Sector III, Salt Lake, Kolkata 700 098, India

[‡]Department of Chemistry, Indian Institute of Technology Madras, Chennai 600 036 India

Supporting Information

ABSTRACT: A one-pot synthesis of extremely stable, water-soluble Cu quantum clusters (QCs) capped with a model protein, bovine serum albumin (BSA), is reported. From matrix-assisted laser desorption ionization time-of-flight (MALDI-TOF) mass spectrometry, we assign the clusters to be composed of Cu_5 and Cu_{13} cores. The QCs also show luminescence properties having excitation and emission maxima at 325 and 410 nm, respectively, with a quantum yield of 0.15, which are found to be different from that of protein alone in similar experimental conditions. The quenching of luminescence of the protein-capped Cu QCs in the presence of very low hydrogen peroxide concentration (approximately nanomolar, or less than part-per-billion) reflects the efficacy of the QCs as a potential sensing material in biological environments. Moreover, as-prepared Cu QCs can detect highly toxic Pb^{2+} ions in water, even at the part-per-million level, without suffering any interference from other metal ions.

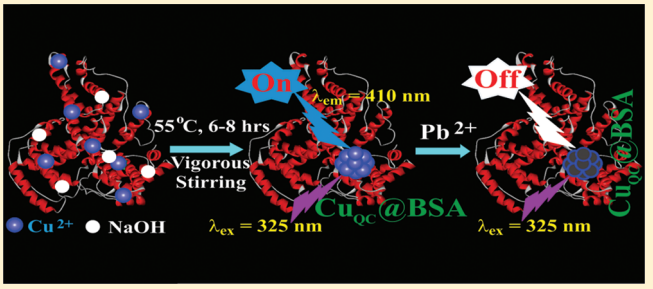

The drive toward optoelectronic nanodevices,[1] biosensors,[2] bioimaging,[3] nanoelectronics,[4] and novel catalysts[5] has generated a need to synthesize new metal clusters. Compared to bulk materials, clusters are of fundamental interest due to their own intrinsic properties but also because of their intermediate position between molecular and materials science. Owing to their ultrasmall size, biocompatibility, and highly luminescent properties, applications of these luminescent quantum clusters would be an attractive field to study. In the past few years, extensive studies have been performed on luminescent Au and Ag nanoclusters[6−10] using various templates such as peptides,[11] DNA,[12] thiols,[13] dendrimers,[14] polymers,[15] and proteins.[6] Among all of them, the use of a biomolecule as template or scaffold for synthesis possesses many advantages in biological applications. However, to date, only a few experimental studies have given direct insight into copper nanoclusters,[16−18] primarily because of the difficulty in preparing highly stable and extremely tiny Cu particles. Additionally, subnanometer-sized Cu intrinsically suffers from unstable colloidal dispersion of its particles and easy surface oxidation on exposure to air. Therefore, it would be of great interest to develop very stable, highly luminescent, biocompatible copper quantum clusters (Cu QCs) with emission in the visible range.

Herein, we report the synthesis of Cu QCs by a simple one-pot chemical reduction method by using a commercially available protein, bovine serum albumin (BSA). It has been demonstrated that BSA can be used as the model protein for the synthesis and stabilization of gold nanoclusters.[6] The resulting Cu QCs were highly resistant to oxidation and exhibit photoluminescence and highly stable properties in a colloidal dispersion. The as-prepared blue-emitting clusters were assigned a molecular formula based on matrix-assisted laser desorption ionization mass spectrometry (MALDI MS). The as-synthesized quantum clusters were characterized thoroughly using various spectroscopic and microscopic techniques [UV−vis, luminescence, transmission electron microscopy (TEM), dynamic light scattering (DLS), X-ray photoelectron spectroscopy (XPS), matrix-assisted laser desorption ionization time-of-flight (MALDI-TOF), thermogravimetric analysis (TGA), and differential scanning calorimetry (DSC)]. The effect of oxidizing agent on the luminescence property of the cluster solution was probed. The luminescence of the QCs was exploited as a selective sensor for the detection of the toxic Pb^{2+} ion. The reason of quenching was found to be aggregation manifested as revealed from our DLS study. To the best of our knowledge this is the first time protein-protected Cu QCs have been synthesized in a protein matrix and used as toxic metal ion sensor at part-per-million levels even in the presence of other interfering ions.

Received: October 1, 2011
Accepted: November 3, 2011
Published: November 03, 2011

EXPERIMENTAL SECTION

Materials. BSA, $CuSO_4$ as well as all the nitrates and chlorides of various metal ions were obtained from Sigma. Sinapinic acid was used as the matrix for MALDI-TOF MS. Millipore water was used throughout the experiments. All chemicals were used as received without further purification.

Synthesis of Cu_{QC}@BSA. In our experiment, aqueous $CuSO_4$ solution (1 mL, 20 mM) was added to BSA solution (5 mL, 15 mg/mL). The solution was stirred at room temperature for 2−3 min, and then NaOH solution was introduced so that pH 12 is achieved. The color of the solution changed from blue to violet within 2−5 min. Finally, the mixture was allowed to stir for 6−8 h at 55 °C, and the color changes to light brown. It has to be noted that formation of the Cu QCs at room temperature is possible; however, more time (48 h) is needed compared to that at 55 °C (6−8 h). It is crucial to know the key parameters such as concentration, pH, and temperature to obtain a high concentration of Cu QCs. Hence, a series of control experiments have been performed (see the Supporting Information, Figures S1−S3). These results indicate that luminescence intensity was high for the reaction with 20 mM $CuSO_4$ solution at pH ∼ 12. We have used these pH and concentration values for synthesizing larger amounts of clusters.

Quantum Yield Calculation. Q_D, the quantum yield of the donor in the absence of an acceptor, was calculated according to the following equation:[19]

$$Q = Q_R\left(\frac{I}{I_R}\right)\left(\frac{OD_R}{OD}\right)\left(\frac{n^2}{n_R{}^2}\right) \quad (1)$$

where Q and Q_R are the quantum yields of the protein and reference [kynurenine in dimethyl sulfoxide (DMSO)], I and I_R are the integrated fluorescence intensities of the protein and reference, OD and OD_R are the optical densities of the protein and reference at the excitation wavelength, and n and n_R are the refractive indexes of the protein and reference solutions. The absolute quantum yield of kynurenine[20] in DMSO was taken to be 0.09.

Characterization. Steady-state absorption and emission were measured with a Shimadzu UV-2450 spectrophotometer and Jobin Yvon Fluoromax-3 fluorimeter, respectively. DLS measurements were done with a Nano S Malvern instrument employing a 4 mW He−Ne laser (λ = 632.8 nm) equipped with a thermostated sample chamber. All the scattered photons are collected at 173° scattering angle. The scattering intensity data are processed using the instrumental software to obtain the hydrodynamic diameter (d_H) and the size distribution of the scatterer in each sample. The instrument measures the time-dependent fluctuation in the intensity of light scattered from the particles in solution at a fixed scattering angle. Hydrodynamic diameter (d_H) of the proteins is estimated from the intensity autocorrelation function of the time-dependent fluctuation in intensity. d_H is defined as

$$d_H = \frac{k_b T}{3\pi\eta D} \quad (2)$$

where k_b is the Boltzmann constant, η is the viscosity, and D is the translational diffusion coefficient. In a typical size distribution graph from the DLS measurement, the X-axis shows a distribution of size classes in nanometers, while the Y-axis shows the relative intensity of the scattered light. Fluorescence decay transients

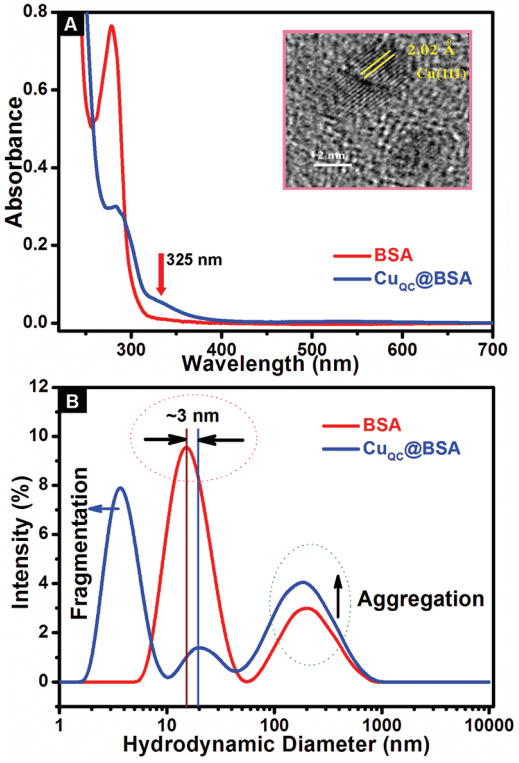

Figure 1. (A) UV−vis absorption spectra of BSA (red line) and Cu_{QC}@BSA solution (blue line). Inset: HRTEM of Cu QCs after being exposed to the electron beam. (B) DLS spectra of BSA (red) and Cu_{QC}@BSA (blue). All the parameters are same in both cases.

were measured and fitted by using a commercially available spectrophotometer (LifeSpec-ps, Edinburgh Instruments, U.K.) with an 60 ps instrument response function (IRF). The observed fluorescence transients are fitted by using a nonlinear least-squares fitting procedure to a function ($X(t) = \int_0^t E(t')R(t - t')\,dt'$) comprising a convolution of the IRF ($E(t)$) with a sum of exponentials ($R(t) = A + \Sigma_{i=1}^{n} B_i e^{-t/\tau_i}$) with pre-exponential factors (B_i), characteristic lifetimes (τ_i), and a background (A). Relative concentration in a multiexponential decay is finally expressed as follows: $c_n = B_n/\Sigma_{i=1}^{n} B_i \times 100$. The quality of the curve fitting is evaluated by reduced χ^2 and residual data. It has to be noted that, with our time-resolved instrument, we can resolve at least one-fourth of the instrument response time constants after the deconvolution of the IRF. The CD spectrum was measured in a Jasco 815 spectropolarimeter with a Peltier setup for the temperature-dependent measurements. CD studies were done with 10 mm path length cell. MALDI MS studies were conducted using a Voyager-DE PRO Biospectrometry workstation from Applied Biosystems. A pulsed nitrogen laser of 337 nm was used for the MALDI MS studies. Mass spectra were collected in positive-ion mode and were averaged for 100 shots. TEM and XPS were performed on an FEI TecnaiTF-20 field-emission high-resolution transmission electron microscope at 200 kV and on a Omicron ESCA probe spectrometer with polychromatic Mg Kα X-rays ($h\nu$ = 1253.6 eV), respectively. The samples were spotted as drop-cast films on a sample stub. A constant analyzer energy of 20 eV was used for the measurements. TGA and DSC were performed on a Perkin-Elmer Diamond TG/DTA and Perkin-Elmer DSC, respectively, at a heating rate of 20 °C/min in

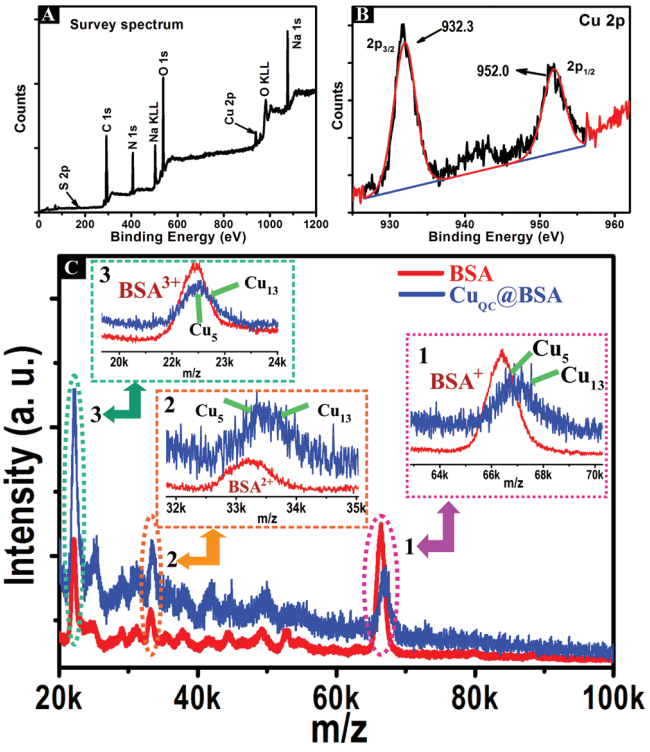

Figure 2. (A) XPS survey spectrum of Cu_{QC}@BSA (black). (B) XPS spectrum in the Cu 2p region of Cu_{QC}@BSA. (C) MALDI-TOF mass spectra of BSA (red) and Cu_{QC}@BSA (blue). The peaks due to singly, doubly, and triply charged ions of Cu_{QC}@BSA are expanded in the inset.

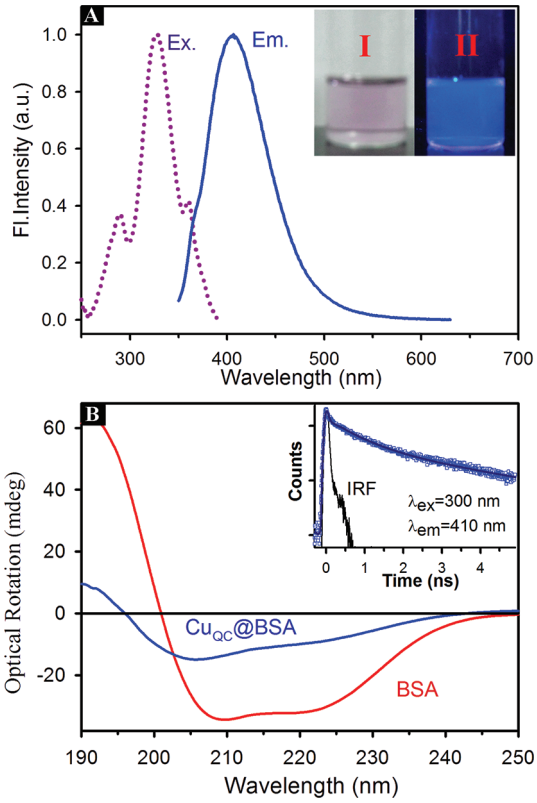

Figure 3. (A) Excitation and emission spectra of Cu_{QC}@BSA at room temperature (pink and blue line). The inset contains the photographs of the Cu_{QC}@BSA under visible light (I) and under UV light (II). (B) Far-UV circular dichroism (CD) spectra of BSA (red) and Cu_{QC}@BSA (blue). Inset: photoluminescence decay of Cu_{QC}@BSA with instrument response function (IRF) ~ 60 ps. Standard errors of decay time components are ~5%.

N_2 atmosphere. Refractive indexes of the solutions are measured by using Rudolph J357 automatic refractometer.

RESULTS AND DISCUSSION

Although weak as compared to the 280 nm peak of pure BSA, a clear absorption spectrum at 325 nm appears in the final solution (Figure 1A). In order to realize the origin of 325 nm peak, we have taken into account any kind of oxidation product of the amino acids in protein. However, it is well-known that all the aromatic amino acids have a characteristic absorption peak ≤280 nm and a few tryptophan metabolites like kynurenine, 3-hydroxykynurenine, and *N*-formylkynurenine have an absorption peak above 300 nm. Our earlier extensive studies confirmed that kynurenine[21] and its derivatives[22] in proteins have a distinct UV−vis peak at above 350 nm. The observed 325 nm absorption peak as well as the emission maxima (see below) revealed in the present study clearly rules out the possibility of any tryptophan metabolites, rather the formation of a new type of material in the protein environment. The high-resolution TEM (HRTEM) images (inset of Figure 1A) showed that the average size is 2.8 ± 0.5 nm where the crystal lattice fringes are 2.02 Å apart which indicates the (111) planes of the metallic Cu (see the Supporting Information, Figure S4). This is not surprising because clusters may fuse to form crystals in the presence of strong electron beam irradiation.[23] Swelling of the protein size as revealed from DLS measurement indicates the formation of a new species inside the protein having size about ~3 nm. Protein fragmentation as well as enhancement of aggregation is also shown in Figure 1B. Recently, it has been reported that fragmentation of protein can occur when the pH of the environment changes drastically.[24] It is also well-established that protein coordinates with copper ion to form aggregates.[25]

XPS analysis is carried out to determine the oxidation state of copper in the samples. Two intense peaks are observed at 932.3 and 952.0 eV (Figure 2B), which are assigned to $2p_{3/2}$ and $2p_{1/2}$ features of Cu(0). Although the lack of a satellite feature is assured in the Figure 2B, a shake-up can be observed at 942 eV, suggesting very minimal presence of Cu(II) in the system. It is also worth mentioning that the $2p_{3/2}$ binding energy of Cu(0) is only ~0.1 eV different from that of Cu(I). Therefore, the valence state of the Cu in protein matrix most likely lies between 0 and +1. Previous studies confirmed that, in gold clusters, atoms can have different oxidation states depending on their position inside the clusters.[26,27] All other expected elements are seen in the survey spectrum (Figure 2A).

As-synthesized material has been studied using MALDI-TOF mass spectrometry to understand the number of copper atoms in the cluster core. The mass spectrum of BSA showed a major peak at around 66 400 Da due to the monocation, which agrees with previous results on Ag_{15} clusters[28] (Figure 2C, inset 1). The Cu cluster containing BSA showed two distinct, but low-intensity peaks at m/z 66 723 and 67 228 Da besides the parent protein peak. The difference between the above peaks with the host protein spectrum measured at pH 12 may be attributed to the 5 and 13 copper atoms, respectively; we assign the clusters to be Cu_5 and Cu_{13}. The presence of doubly as well as triply charged

dx.doi.org/10.1021/ac202610e |*Anal. Chem.* 2011, 83, 9676–9680

clusters along with the corresponding peaks of the protein observed in the MALDI MS data clearly indicates that the Cu cluster is associated with a single protein molecule (see Figure 2C, insets 2 and 3). From all the data presented so far, we conclude that the copper quantum clusters (Cu QCs) are formed within BSA and would be referred as Cu_{QC}@BSA henceforth.

The luminescence of Cu_{QC}@BSA revealing distinct excitation and emission maxima at 325 and 410 nm, respectively, is evident from Figure 3A. The peak position (325 nm) of the excitation spectrum is almost alike to the Cu QCs absorption band in Figure 1A. As the reaction progressed, a gradual increase in the luminescence from the solution has been observed (Supporting Information Figure S5). After around 6−8 h of reaction, there is no further enhancement in the luminescence and the reaction is considered to be terminated. Moreover, for 325 nm excitation, the integrated fluorescence quantum yield for Cu_{QC}@BSA is 0.15 using kynurenine as the reference. Protein alone shows insignificant emission upon 325 nm excitation at pH 12 (see Supporting Information Figure S6) confirming the absence of emitting amino acid metabolites. At this juncture it is important to mention that we have checked the possibility of interfering luminescence from the protein matrix in a similar experimental condition. The yield is found to be 2×10^{-2} with no specific absorption and emission maxima. This observation clearly rules out the possible interference in the measured luminescence for the Cu_{QC}@BSA complex. The luminescence decay of the Cu_{QC}@BSA in water is measured by a picosecond-resolved time-correlated single-photon counting (TCSPC) technique (inset of Figure 3B). The decay profile of the Cu_{QC}@BSA is monitored at an excitation wavelength of 300 nm. The numerical fitting of the luminescence collected at 410 nm reveals time constants of 0.03 ns (78%), 0.71 ns (15%), and 3.5 ns (7%), which may be due to the electronic transitions between "sp" conduction band and filled "d^{10}" band.

This Cu_{QC}@BSA has a photoluminescence (PL) peak at ~410 nm, indicating the presence of Cu_{13} quantum clusters based on our estimation using the spherical Jellium model;[29] i.e., $E_g = E_{fermi}/N^{1/3}$, where E_{fermi} is the Fermi energy of bulk material and N is the number of atoms per cluster, which also supports our MALDI MS data. Theoretical calculations[29] and all the above-mentioned observations from UV−vis, PL, lifetime, MALDI MS, and XPS investigations indicate the formation of Cu QCs. Nevertheless, in order to further confirm the formation of QCs, as some aromatic amino acid metabolites are also known to emit in the blue region, we have performed the following experiments. In the presence of an oxidizing agent, Cu QCs, if present, would be oxidized and should result in quenching of its luminescence and optical absorption. However, if the blue luminescence originates from the oxidized product of protein then it would expect to increase. We have added H_2O_2 of different concentrations to the as-synthesized Cu QCs, and we notice concentration-dependent quenching of luminescence, which further corroborates the presence of Cu QCs in the protein matrix (Supporting Information Figures S7 and S8). From an application point of view, it can be used as a H_2O_2 sensor in the nanomolar level. In contrast, the control protein solution does not provide any luminescence enhancement upon addition of H_2O_2 which rules out the possibility of oxidized product of protein. TGA and DSC studies on other metal clusters are found to be very informative about the formation of cluster in protein and thiol matrixes.[6,30] Our TGA and DSC studies of BSA and

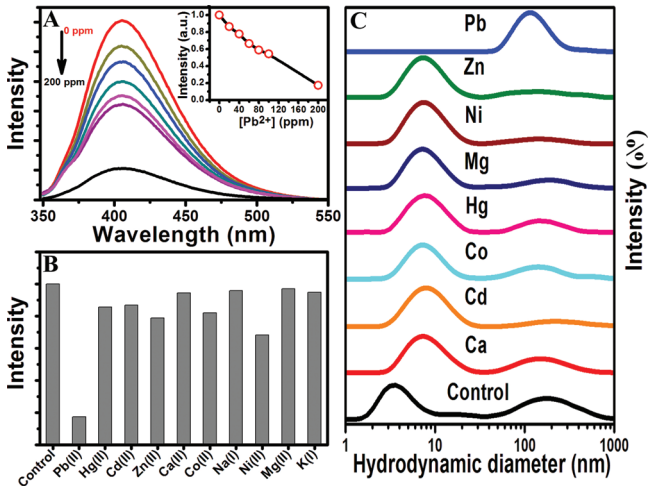

Figure 4. (A) Luminescence responses of Cu_{QC}@BSA after the addition of Pb^{2+} ion (0−200 ppm). Inset: plot of the luminescence peak intensity vs the concentration of Pb^{2+} ion. (B) Selectivity of the Cu_{QC}@BSA to different metal ions. The luminescence intensities were recorded at 406 nm. For panel B, the final metal ion concentrations are 200 ppm. (C) DLS spectra of Cu_{QC}@BSA solution in the absence (control) and presence of different metal ions.

Cu_{QC}@BSA also provided supporting evidence for the formation of the QCs (Supporting Information Figure S10).

The obtained Cu QCs are found to be very stable, showing the same emission spectra after almost 2 months of being stored at room temperature (Supporting Information Figure S11). The emission peak remains unchanged at pH 7−12, as can be seen in Supporting Information Figure S12. In order to investigate the thermal stability of the QCs, temperature-dependent luminescence of Cu_{QC}@BSA has been monitored. It can be seen from Supporting Information Figure S13 that emission of the Cu_{QC}@BSA in the aqueous solution decreased significantly upon increase in temperature. The reason may be the increase in hydrophilicity around the Cu QCs as protein is perturbed at higher temperature (which is also reflected in circular dichroism (CD) measurements, see Supporting Information Figure S14). The minor red shift of the position of luminescence maximum with temperature is due to the relative strengths of ground- and excited-state solvent stabilization. We have employed the CD method to study the conformational behavior of BSA before and after the formation of the Cu QCs. Native BSA displays CD features with minima at 208 and 222 nm, corresponding to the secondary structure of the protein (Figure 3B). However, after the formation of Cu QCs, the 208 nm peak is shifted to 204 nm indicating the loss of α-helix content and increase in β-sheet and random coil structures. The percentage of various conformations has been determined for both pure BSA and Cu_{QC}@BSA by using CDNN software, which revealed 15% loss of α-helix structure.

The luminescence of the as-prepared Cu_{QC}@BSA can be used as a highly sensitive and selective luminescence "turn-off" sensor for the Pb^{2+} ion. We found that the luminescence of Cu QCs is quenched in the presence of Pb^{2+} ion. It can be seen from the Figure 4A that more and more quenching occurs with an increase in Pb^{2+} ion. Herein, we have also carried out studies with other metal ions, such as Hg^{2+}, Ca^{2+}, Co^{2+}, Zn^{2+}, Ni^{2+}, Cd^{2+}, Mg^{2+}, Na^{+}, and K^{+}, under exactly similar conditions that were used for the detection of Pb^{2+} ion. Chlorides and nitrates of the metals are

used. Metal ions are added to aqueous solutions of the Cu QCs such that the final concentration was 200 ppm, and the luminescence of the Cu QCs is measured immediately after the addition of ions. However, no such quenching effect like that of the Pb^{2+} ion is observed. The relative luminescence quenching of Cu_{QC}@BSA toward various common metal ions is presented in Figure 4B. This result suggests that our luminescent Cu QCs are selective for Pb^{2+} detection. The luminescence quenching in the presence of Pb^{2+} can be attributed to the QC aggregation induced by the complexation between BSA and the Pb^{2+} ion. BSA contains a high-affinity site for Pb^{2+} ion; the binding involves carboxylate groups. To explore the quenching mechanism, we have performed a DLS measurement. It can be seen from Figure 4C that only Pb^{2+} ion can induce the protein−protein interaction which leads to spherical aggregation of Cu_{QC}@BSA. We have also checked the efficacy of Pb^{2+} ion detection in presence of other metal ions (Hg^{2+}, Ca^{2+}, Co^{2+}, Zn^{2+}, Ni^{2+}, Cd^{2+}, Mg^{2+}, Na^{+}, and K^{+}) of similar concentrations. As shown in Supporting Information Figure S15 the Cu QCs reveal significant efficacy in the detection of Pb^{2+} ion even in presence of other metal ions.

CONCLUSION

In summary, we have reported a method for preparing highly stable, blue luminescent, and water-soluble Cu QCs using a common protein, BSA. It can selectively and very sensitively detect highly toxic lead ions at part-per-million concentrations even in the presence of other interfering ions. This study would be potentially extended to generate other quantum clusters and applied as a good candidate for biolabeling, biosensing, and applications in material and biomaterial sciences.

ASSOCIATED CONTENT

Supporting Information. Detailed experimental procedures, UV−vis, MALDI MS, XPS, HRTEM, TGA, DSC, TCSPC, CD data, and photoluminescence measurements. This material is available free of charge via the Internet at http://pubs.acs.org.

AUTHOR INFORMATION

Corresponding Author

*E-mail: skpal@bose.res.in (S.K.P.); pradeep@IITM.AC.IN (T.P.).

ACKNOWLEDGMENT

N.G. thanks CSIR, India, for a fellowship. A.G. thanks UGC, India, for a fellowship. We thank DST for a financial Grant (SR/SO/BB-15/2007). Equipment support to T.P. was provided by the Nano Mission of DST, Government of India.

REFERENCES

(1) Alivisatos, A. P. *Science* **1996**, *271*, 933.
(2) Elghanian, R.; Storhoff, J. J.; Mucic, R. C.; Letsinger, R. L.; Mirkin, C. A. *Science* **1997**, *277*, 1078.
(3) Polavarapu, L.; Manna, M.; Xu, Q. H. *Nanoscale* **2011**, *3*, 429.
(4) Schmid, G. *Adv. Eng. Mater.* **2001**, *3*, 737.
(5) Zhu, Y.; Qian, H. F.; Jin, R. C. *Chem.—Eur. J.* **2010**, *16*, 11455.
(6) Xie, J. P.; Zheng, Y. G.; Ying, J. Y. *J. Am. Chem. Soc.* **2009**, *131*, 888.
(7) Zheng, J.; Nicovich, P. R.; Dickson, R. M. *Annu. Rev. Phys. Chem.* **2007**, *58*, 409.
(8) Lan, G. Y.; Huang, C. C.; Chang, H. T. *Chem. Commun.* **2010**, *46*, 1257.
(9) Rao, T. U. B.; Nataraju, B.; Pradeep, T. *J. Am. Chem. Soc.* **2010**, *132*, 16304.
(10) Xavier, P. L.; Chaudhari, K.; Verma, P. K.; Pal, S. K.; Pradeep, T. *Nanoscale* **2010**, *2*, 2769.
(11) Slocik, J. M.; Wright, D. W. *Biomacromolecules* **2003**, *4*, 1135.
(12) Petty, J. T.; Zheng, J.; Hud, N. V.; Dickson, R. M. *J. Am. Chem. Soc.* **2004**, *126*, 5207.
(13) Wu, Z.; Lanni, E.; Chen, W.; Bier, M. E.; Ly, D.; Jin, R. *J. Am. Chem. Soc.* **2009**, *131*, 16672.
(14) Tanaka, S.-I.; Miyazaki, J.; Tiwari, D. K.; Jin, T.; Inouye, Y. *Angew. Chem., Int. Ed.* **2011**, *50*, 431.
(15) Tam, J. M.; Tam, J. O.; Murthy, A.; Ingram, D. R.; Ma, L. L.; Travis, K.; Johnston, K. P.; Sokolov, K. V. *ACS Nano* **2010**, *4*, 2178.
(16) Wei, W. T.; Lu, Y. Z.; Chen, W.; Chen, S. W. *J. Am. Chem. Soc.* **2011**, *133*, 2060.
(17) Vilar-Vidal, N.; Blanco, M. C.; Lopez-Quintela, M. A.; Rivas, J.; Serra, C. *J. Phys. Chem. C* **2010**, *114*, 15924.
(18) Kawasaki, H.; Kosaka, Y.; Myoujin, Y.; Narushima, T.; Yonezawa, T.; Arakawa, R. *Chem Commun.* **2011**, *47*, 7740.
(19) Chen, J.; Flaugh, S. L.; Callis, P. R.; King, J. *Biochemistry* **2006**, *45*, 11552.
(20) Sherin, P. S.; Grilj, J.; Tsentalovich, Y. P.; Vauthey, E. *J. Phys. Chem. B* **2009**, *113*, 4953.
(21) Goswami, N.; Makhal, A.; Pal, S. K. *J. Phys. Chem. B* **2010**, *114*, 15236.
(22) Si, S.; Mandal, T. K. *Chem.—Eur. J.* **2007**, *13*, 3160.
(23) Ramasamy, P.; Guha, S.; Sidharth Shibu, E.; Sreeprasad, T. S.; Bag, S.; Banerjee, A.; Pradeep, T. *J. Mater. Chem.* **2009**, *19*, 8456.
(24) Chaudhari, K.; Lourdu Xavier, P.; Pradeep, T. *ACS Nano* **2011**, *5*, 8816–8827.
(25) Drew, S. C.; Barnham, K. J. *Acc. Chem. Res.* **2011**, *44*, 1146.
(26) Whetten, R. L.; Price, R. C. *Science* **2007**, *318*, 407.
(27) Akola, J.; Walter, M.; Whetten, R. L.; Hakkinen, H.; Gronbeck, H. *J. Am. Chem. Soc.* **2008**, *130*, 3756.
(28) Mathew, A.; Sajanlal, P. R.; Pradeep, T. *J. Mater. Chem.* **2011**, *21*, 11205.
(29) Zheng, J.; Zhang, C. W.; Dickson, R. M. *Phys. Rev. Lett.* **2004**, *93*, 409.
(30) Zhu, M.; Lanni, E.; Garg, N.; Bier, M. E.; Jin, R. *J. Am. Chem. Soc.* **2008**, *130*, 1138.